

temperatures is favored for this type of adsorption, it increases with the increase of temperatures. For example, materials that contain silica aluminates or calcium oxide such as silica sand, kaolinite, bauxite, limestone, and aluminum oxide, were used as sorbents to capture heavy metals at high temperatures. The adsorption efficiency of the sorbents are influenced by operating temperature [2-7]. Usually, the removal of the chemisorbed species from the surface may be possible only under extreme conditions of temperature or high vacuum, or by some suitable chemical treatment of the surface. In deed, the chemisorption process depends on the surface area [8]. It too increases with an increase of surface area because the adsorbed molecules are linked to the surface by valence bonds. Normally, the chemi-adsorbed material forms a layer over the surface, which is only one chemisorbed molecule thick, *i.e.* they will usually occupy certain *adsorption sites* on the surface, and the molecules are not considered free to move from one surface site to another [9]. When the surface is covered by the monomolecular layer (monolayer adsorption), the capacity of the adsorbent is essentially exhausted. In addition, this type of adsorption is irreversible [10], wherein the chemical nature of the adsorbent(s) may be altered by the surface dissociation or reaction in which the original species cannot be recovered *via* desorption process [11]. In general, the adsorption isotherms indicated two distinct types of adsorption—reversible (composed of both physisorption and weak chemisorption) and irreversible (strongly chemisorbed) [10-11].

On the other hand *Physisorption* is a physical adsorption involving intermolecular forces (Van der Waals forces), which do not involve a significant change in the electronic orbital patterns of the species [12]. The energy of interaction between the adsorbate and adsorbent has the same order of magnitude as, but is usually greater than the energy of condensation of the adsorptive. Therefore, no activation energy is needed. In this case, low temperature is favourable for the adsorption. Therefore, the *physisorption* decreases with increase temperatures [13]. In physical adsorption, equilibrium is established between the adsorbate and the fluid phase resulting multilayer adsorption. Physical adsorption is relatively non specific due to the operation of weak forces of attraction between molecules. The adsorbed molecule is not affixed to a particular site on the solid surface, but is free to move about over the surface. Physical adsorption is generally is reversible in nature; *i.e.*, with a decrease in concentration the material is desorbed to the same extent that it was originally adsorbed [14]. In this case, the adsorbed species are chemically identical with those in the fluid phase, so that the chemical nature of the fluid is not altered by adsorption and subsequent desorption; as result, it is not specific in nature. In addition, the adsorbed material may condense and form several superimposed layers on the surface of the adsorbent [15].

Some times, both physisorption and chemisorption may occur on the surface at the same time, a layer of molecules may be physically adsorbed on a top of an underlying chemisorbed layer [16].

In summary, based on the different reversibility and specific of physical and chemical adsorption processes, thermal desorption of the adsorbed sorbent could provide important information for the study of adsorption mechanism.

2. Factors affecting adsorption

In general, the adsorption reaction is known to proceed through the following three steps [16]:

1. Transfer of adsorbate from bulk solution to adsorbent surface, which is usually mentioned as diffusion.
2. Migration of adsorbate (Fe^{3+} ion, where its ionic radius = 0.064 nm) into pores.
3. Interaction of Fe^{3+} ion with available sites on the interior surface of pores.

From the previous studies, it was shown that the rate-determining step for the adsorption of Fe^{3+} ion is step (3).

Normally, the driving force for the adsorption process is the concentration difference between the adsorbate in the solution at any time and the adsorbate in the solution at equilibrium ($C-C_e$) [17]. but, there are some important factors affecting adsorption, such as the factors affecting the adsorption of Fe^{3+} ions in the aqueous solution:

2.1 Surface area of adsorbent

Larger surface area imply a greater adsorption capacity, for example, carbon and activated carbon [18].

2.2 Particle size of adsorbent

Smaller particle sizes reduce internal diffusion and mass transfer limitation to penetrate of the adsorbate inside the adsorbent (i.e., equilibrium is more easily achieved and nearly full adsorption capability can be attained). Figure 2 represents the removal efficiency Fe^{3+} ions by natural zeolite through three different particle sizes (45, 125 and 250 μm). It can be observed that the maximum adsorption efficiency is achieved with particle size 45 μm . This is due to the most of the internal surface of such particles might be utilized for the adsorption. The smaller particle size gives higher adsorption rates, in which the Fe^{3+} ion has short path to transfer inside zeolite pores structure of the small particle size [19].

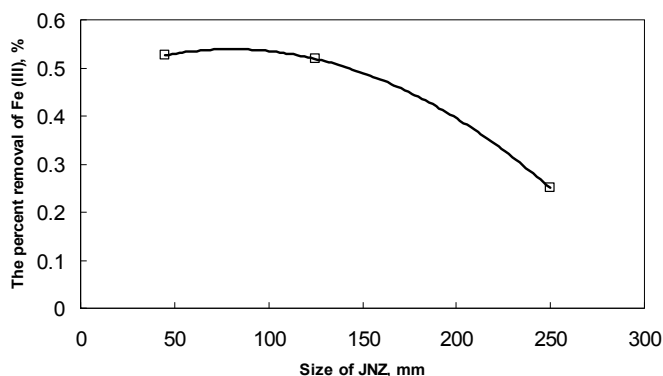


Fig. 2. Percent removal of Fe^{3+} ions (1000 ppm) vs. natural zeolite particle size: 1 g adsorbent/ 50 ml Fe^{3+} ion solution, initial pH of 1% HNO_3 , and 300 rpm.

2.3 Contact time or residence time

The longer residence time means the more complete the adsorption will be. Therefore, the required contact time for sorption to be completed is important to give insight into a sorption process. This also provides an information on the minimum time required for considerable adsorption to take place, and also the possible diffusion control mechanism

between the adsorbate, for example Fe^{3+} ions, as it moves from the bulk solution towards the adsorbent surface, for example natural zeolite [19].

For example, the effect of contact time on sorption of Fe^{3+} ions is shown in Figure 3. At the initial stage, the rate of removal of Fe^{3+} ions using natural quartz (NQ) and natural bentonite (NB) is higher with uncontrolled rate. The initial faster rate may be due to the availability of the uncovered surface area of the adsorbent such as NQ and NB initially [20]. This is because the adsorption kinetics depends on: (i) the surface area of the adsorbent, (ii) the nature and concentration of the surface groups (active sites), which are responsible for interaction with the Fe^{3+} ions. Therefore, the adsorption mechanism on both adsorbent has uncontrolled rate during the first 10 minutes, where the maximum adsorption is achieved. Afterward, at the later stages, there is no influence for increasing the contact time. This is due to the decreased or lesser number of active sites. Similar results have been shown in our results using zeolite and olive cake as well as other reported in literatures for the removal of dyes, organic acids and metal ions by various adsorbents [19, 21].

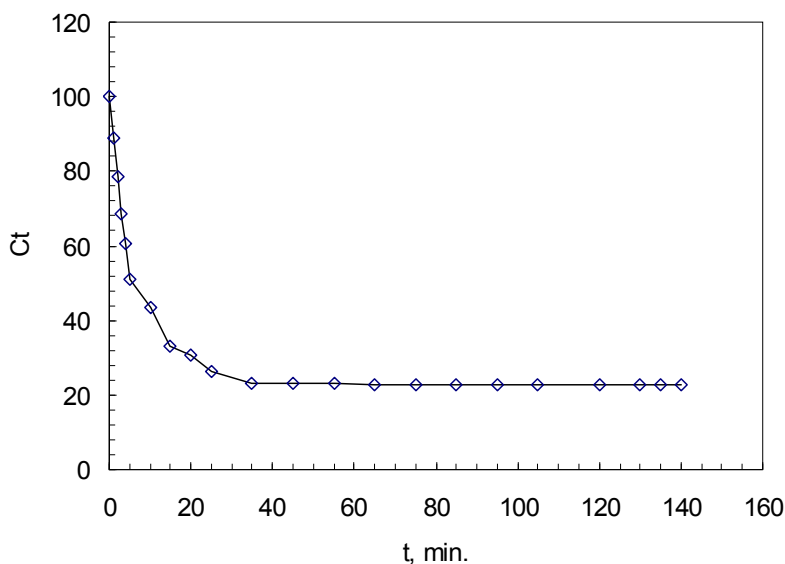


Fig. 3. Adsorption of Fe^{3+} ions onto olive cake. Variation of the Fe^{3+} ions concentration with time. (Initial concentration of Fe^{3+} ions: 100 ppm, Agitation speed: 100 rpm, pH: 4.5, temperature 28 °C).

2.4 Solubility of adsorbent/ heavy metals in wastewater/ water

The slightly soluble metal ions in water will be more easily removed from water (i.e., adsorbed) than substances with high solubility. Also, non-polar substances will be more easily removed than polar substances since the latter have a greater affinity for adsorption.

2.5 Affinity of the solute for the adsorbent

If the surface of adsorbent is slightly polar, the non-polar substances will be more easily picked up by the adsorbent than polar ones (the opposite is correct).

2.6 Size of the molecule with respect to size of the pores

Large molecules may be too large to enter small pores. This may reduce adsorption independently of other causes.

2.7 Degree of ionization of the adsorbate molecule

More highly ionized molecules are adsorbed to a smaller degree than neutral molecules.

2.8 pH

The degree of ionization of a species is affected by the pH (e.g., a weak acid or a weak basis). This, in turn, affects adsorption. For example, the precipitation of Fe^{3+} ions occurred at pH greater than 4.5 (see Figure 4). The decrease in the Fe^{3+} ions removal capacity at pH > 4.5 may have been caused by the complexing Fe^{3+} ions with hydroxide. Therefore, the removal efficiency increases with increasing initial pH. For example, at low pH, the concentration of proton is high. Therefore, the positively charged of the Fe^{3+} ions and the protons compete for binding on the adsorbent sites in Zeolite, Bentonite, Quartz, olive cake, Tripoli in which, this process decrease the uptake of iron ions. The concentration of proton in the solution decrease as pH gradually increases in the ranges from 2 to 4.5. In this case, little protons have the chance to compete with Fe^{3+} ions on the adsorption sites of the olive cake. Thus, higher pH in the acidic media is facilitated the greater uptake of Fe^{3+} ions. Above pH 4.5, the removal efficiency decreases as pH increases, this is inferred to be attributable to the hydrolysis [19-22].

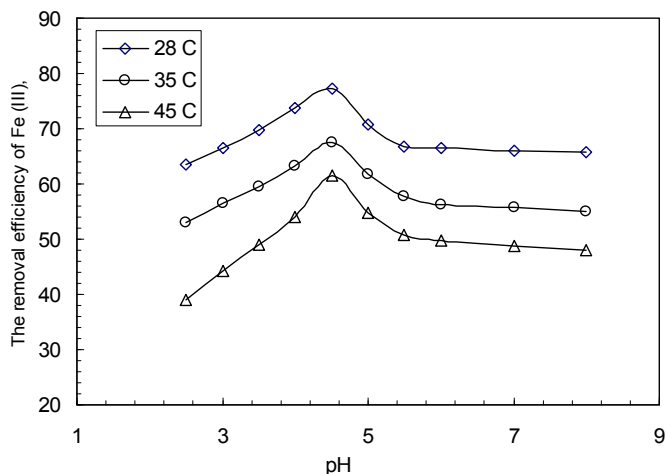


Fig. 4. Effect of initial pH on the removal efficiency, %, of Fe^{3+} ions at different temperatures. (Initial concentration of Fe^{3+} ions: 100 ppm, Agitation speed: 100 rpm, Mass of olive cake: 1 g, Dose: 5 g/l, Contact time: 24 hr).

2.9 Effect of initial concentration

At high-level concentrations, the available sites of adsorption become fewer. This behaviour is connected with the competitive diffusion process of the Fe^{3+} ions through the micro-

channel and pores in NB [20]. This competitive will lock the inlet of channel on the surface and prevents the metal ions to pass deeply inside the NB, *i.e.* the adsorption occurs on the surface only. These results indicate that energetically less favorable sites by increasing metal concentration in aqueous solution. This results are found matching with our recently studies using natural zeolite [19] and olive cake [21], in addition to other reported by Rao *et al.* [23] and Karthikeyan *et al.* [24]. The removal efficiency of Fe^{3+} ions on NQ and NB as well as zeolite at different initial concentrations (50, 100, 200, 300 and 400 ppm) is shown in the Figures 5-6. It is evident from the figure that the percentage removal of Fe^{3+} ions on NQ is slightly depended on the initial concentration. While the removal efficiency of Fe^{3+} ions using NB decreases as the initial concentration of Fe^{3+} ions increases. For example, the percentage removal is calculated 98 % using the initial concentration of 50 ppm, while it is found 28 % using high-level of 400 ppm [20].

On the other hand, it is clear from Figure 6 that the removal efficiency of Fe^{3+} ions using NQ is less affected by the initial concentration. For instance, the percentage removal using 50 ppm of the initial concentration is found 35 %, while is found 34.9 % using high-level concentrations (400 ppm). This means that the high concentration of Fe^{3+} ions will create and activate of some new activation sites on the adsorbent surface [20, 25].

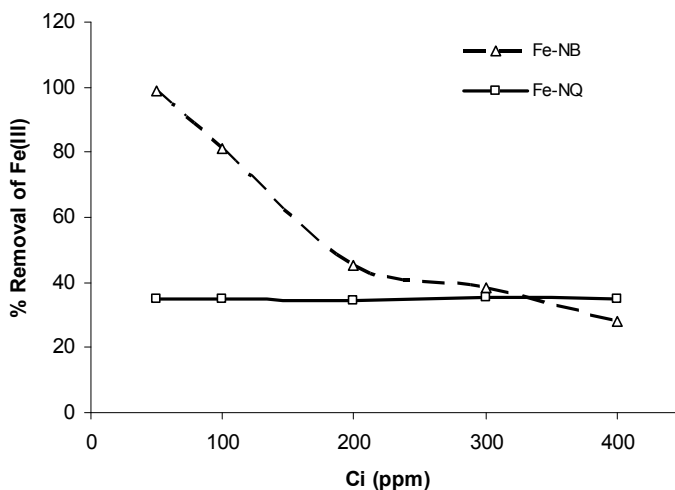


Fig. 5. The effect of initial concentration namely 50, 100, 200, 300 and 400 ppm of Fe^{3+} ions at constant contact time (2.5 hours), adsorbent dosage 4 g/L of natural NQ and NB, Temperature (30 °C) and agitation speed (300 rpm).

2.10 Dosage effect

The removal efficiency is generally increased as the concentration dose increases over these temperature values. This can be explained by the fact that more mass available, more the contact surface offered to the adsorption. The effect of the Jordanian Natural Zeolite (JNZ) dosage on the removal of Fe^{3+} ions is shown in Figure 6 [19]. The adsorbent dosage is varied from 10 to 40 g/l. The initial Fe^{3+} ions concentration, stirrer speed, initial pH and temperature are 1000 ppm, 300 rpm, 1% HNO_3 , and 30 °C, respectively. This figure shows that the maximum removal of 69.15 % is observed with the dosage of 40 g/l. We observed

that the removal efficiency of adsorbents generally improved with increasing amount of JNZ. This is expected because the higher dose of adsorbent in the solution, the greater availability of exchangeable sites for the ions, *i.e.* more active sites are available for binding of Fe^{3+} ions. Moreover, our recent studies using olive cake, natural quartz and natural bentonite and tripoli [19-22] are qualitatively in a good agreement with each other and with those found in the literatures [26].

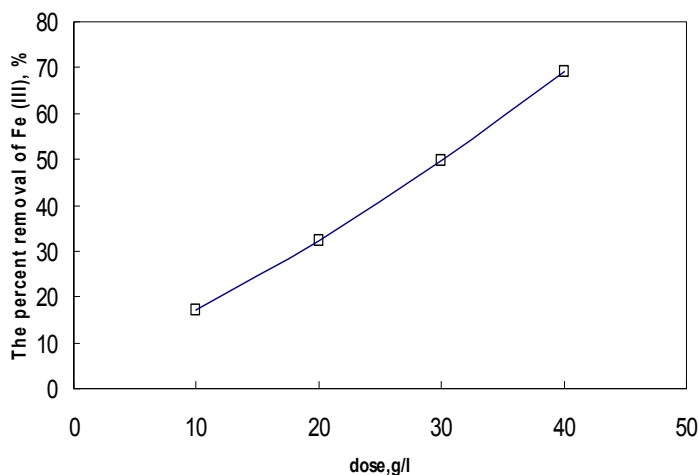


Fig. 6. The adsorbent dose of JNZ vs. Percent removal of Fe^{3+} ions: 1 g adsorbent/ 50 ml Fe^{3+} ions solution, 30 °C, initial pH of 1% HNO_3 , 300 rpm, and constant initial concentration (1000 ppm).

3. Adsorption operation

Adsorption from solution is usually conducted using either the column or the batch operation. It should be possible to characterize the solution - adsorbent system by both technique operations and arrive at the same result. This is due to the physical and/or chemical forces applicable in each case must be identical. Furthermore, the results obtained from the batch experiment should be somewhat more reliable. Among the most serious objections of the column experiments are: (1) the inherent difficulties associated to maintain a constant flow rate; (2) the difficulty of ensuring a constant temperature throughout the column; (3) the appreciable probability of presence the channels within the packed column; and (4) the relatively large expenditure both in time and manpower required for a column experiment.

3.1 Batch operation

In a batch operation, fixed amount of adsorbent is mixed all at once with specific volume of adsorbate (with the range of initial concentration). Afterwards, the system kept in agitation for a convenient period of time. Separation of the resultant solution is accomplished by filtering, centrifuging, or decanting. The optimum pH, contact time, agitation speed and optimum temperature are fixed and used in this technique. For instance, the contact time study, the experiment are carried out at constant initial concentration, agitation speed, pH, and temperature. During the adsorption progress, the mixture container must be covered by

alumina foil to avoid the evaporation. The samples are withdrawn at different time intervals, for example, every 5 minutes or every 15 minutes.

The uptake of heavy metal ions was calculated from the mass balance, which was stated as the amount of solute adsorbed onto the solid. It equal the amount of solute removed from the solution. Mathematically can be expressed in equation 1 [27]:

$$q_e = \frac{(C_i - C_e)}{S} \quad (1)$$

q_e : Heavy metal ions concentration adsorbed on adsorbent at equilibrium (mg of metal ion/g of adsorbent).

C_i : Initial concentration of metal ions in the solution (mg/l).

C_e : Equilibrium concentration or final concentration of metal ions in the solution (mg/l). S : Dosage (slurry) concentration and it is expressed by equation 2:

$$S = \frac{m}{v} \quad (2)$$

Where v is the initial volume of metal ions solution used (L) and m is the mass of adsorbent. The percent adsorption (%) was also calculated using equation 3:

$$\% \text{ adsorption} = \frac{C_i - C_e}{C_i} \times 100\% \quad (3)$$

3.2 Column operation

In a column operation, the solution of adsorbate such as heavy metals (with the range of initial concentration) is allowed to percolate through a column containing adsorbent (ion exchange resin, silica, carbon, etc.) usually held in a vertical position. For instance, column studies were carried out in a column made of Pyrex glass of 1.5 cm internal diameter and 15 cm length. The column was filled with 1 g of dried PCA by tapping so that the maximum amount of adsorbent was packed without gaps. The influent solution was allowed to pass through the bed at constant flow rate of 2 mL/min, in down flow manner with the help of a fine metering valve. The effluent solution was collected at different time intervals.

The breakthrough adsorption capacity of adsorbate (heavy metal ions) was obtained in column at different cycles using the equation 4 [28].

$$q_e = [(C_i - C_e) / m] \times bv \quad (4)$$

Where C_i and C_e denote the initial and equilibrium (at breakthrough) of heavy metal ions concentration (mg/L) respectively. bv was the breakthrough volume of the heavy metal ions solution in liters, and m was the mass of the adsorbent used (g). After the column was exhausted, the column was drained off the remaining aqueous solution by pumping air. The adsorption percent is given by equation 5.

$$\% \text{ Desorption} = (C_e / C_i) \times 100 \quad (5)$$

4. Thermodynamic and adsorption isotherms

Adsorption isotherms or known as equilibrium data are the fundamental requirements for the design of adsorption systems. The equilibrium is achieved when the capacity of the

adsorbent materials is reached, and the rate of adsorption equals the rate of desorption. The theoretical adsorption capacity of an adsorbent can be calculated with an adsorption isotherm. There are basically two well established types of adsorption isotherm the Langmuir and the Freundlich adsorption isotherms. The significance of adsorption isotherms is that they show how the adsorbate molecules (metal ion in aqueous solution) are distributed between the solution and the adsorbent solids at equilibrium concentration on the loading capacity at different temperatures. That mean, the amount of sorbed solute versus the amount of solute in solution at equilibrium.

4.1 Langmuir adsorption isotherm

Langmuir is the simplest type of theoretical isotherms. Langmuir adsorption isotherm describes quantitatively the formation of a monolayer of adsorbate on the outer surface of the adsorbent, and after that no further adsorption takes place. Thereby, the Langmuir represents the equilibrium distribution of metal ions between the solid and liquid phases [29]. The Langmuir adsorption is based on the view that every adsorption site is identical and energetically equivalent (thermodynamically, each site can hold one adsorbate molecule). The Langmuir isotherm assume that the ability of molecule to bind and adsorbed is independent of whether or not neighboring sites are occupied. This mean, there will be no interactions between adjacent molecules on the surface and immobile adsorption. Also mean, trans-migration of the adsorbate in the plane of the surface is precluded. In this case, the Langmuir isotherms is valid for the dynamic equilibrium adsorption – desorption processes on completely homogeneous surfaces with negligible interaction between adsorbed molecules that exhibit the form:

$$q_e = (Q \times b \times C_e) / (1 + b \times C_e) \quad (6)$$

C_e = The equilibrium concentration in solution

q_e = the amount adsorbed for unit mass of adsorbent

Q and b are related to standard monolayer adsorption capacity and the Langmuir constant, respectively.

$$q_{\max} = Q \times b \quad (7)$$

q_{\max} = is the constant related to overall solute adsorptivity (l/g).

Equation 6 could be re-written as:

$$C_e / q_e = 1 / (q_{\max} \times b) + (1 / q_{\max}) \times C_e \quad (8)$$

In summary, the Langmuir model represent one of the the first theoretical treatments of non-linear sorption and suggests that uptake occurs on a homogenous surface by monolayer sorption without interaction between adsorbed molecules. The Langmuir isotherm assumes that adsorption sites on the adsorbent surfaces are occupied by the adsorbate in the solution. Therefore the Langmuir constant (b) represents the degree of adsorption affinity the adsorbate. The maximum adsorption capacity (Q) associated with complete monolayer cover is typically expressed in (mg/g). High value of b indicates for much stronger affinity of metal ion adsorption.

The shape of the isotherm (assuming the (x) axis represents the concentration of adsorbing material in the contacting liquid) is a gradual positive curve that flattens to a constant value.

A plot of C_e/q_e versus C_e gives a straight line of slope $1/q_{\max}$ and intercept $1/(q_{\max} \times b)$, for example, as shown in Figure 4.

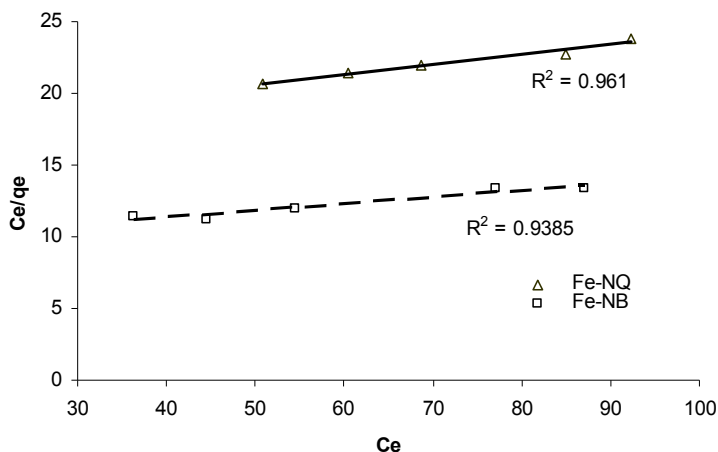


Fig. 4. The linearized Langmuir adsorption isotherms for Fe^{3+} ions adsorption by natural quartz (NQ) and bentonite (NB) at constant temperature 30°C . (initial concentration: 400 ppm, 300 rpm and contact time: 2.5 hours).

The effect of isotherm shape is discussed from the direction of the predicting whether and adsorption system is "favorable" or "unfavorable". Hall et al (1966) proposed a dimensionless separation factor or equilibrium parameter, R_L , as an essential feature of the Langmuir Isotherm to predict if an adsorption system is "favourable" or "unfavourable", which is defined as [30]:

$$R_L = 1/(1+bC_i) \quad (9)$$

C_i = reference fluid-phase concentration of adsorbate (mg/l) (initial Fe^{3+} ions concentration)
 b = Langmuir constant (ml mg^{-1})

Value of R_L indicates the shape of the isotherm accordingly as shown in Table 1 below. For a single adsorption system, C_i is usually the highest fluid-phase concentration encountered.

Value of R_L	Type of Isotherm
$0 < r < 1$	Favorable
$r > 1$	Unfavorable
$r = 1$	Linear
$R = 0$	Irreversible

Table 1. Type of isotherm according to value of R_L

4.2 Freundlich adsorption isotherms

Freundlich isotherm is commonly used to describe the adsorption characteristics for the heterogeneous surface [31]. It represents an initial surface adsorption followed by a condensation effect resulting from strong adsorbate-adsorbate interaction. Freundlich

isotherm curves in the opposite way of Langmuir isotherm and is exponential in form. The heat of adsorption, in many instances, decreases in magnitude with increasing extent of adsorption. This decline in heat is logarithmic implying that the adsorption sites are distributed exponentially with respect to adsorption energy. This isotherm does not indicate an adsorption limit when coverage is sufficient to fill a monolayer ($\theta = 1$). The equation that describes such isotherm is the Freundlich isotherm, given as [31]:

$$q_e = K_f (C_e)^{1/n} \quad n > 1 \quad (10)$$

K_f = Freundlich constant related to maximum adsorption capacity (mg/g). It is a temperature-dependent constant.

n = Freundlich constant related to surface heterogeneity (dimensionless). It gives an indication of how favorable the adsorption processes.

With $n = 1$, the equation reduces to the linear form: $q_e = k \times C_e$

The plotting q_e versus C_e yield a non-regression line, which permits the determination of $(1/n)$ and K_f values of $(1/n)$ ranges from 0 to 1, where the closer value to zero means the more heterogeneous the adsorption surface. On linearization, these values can be obtained by plotting $(\ln q_e)$ versus $(\ln C_e)$ as presented in equation 11. From the plot, the values K_f and n can be obtained.

$$\ln q_e = \ln K_f + (1/n) \ln C_e \quad (11)$$

where, the slope = $(1/n)$, and the intercept = $\ln K_f$

4.3 Dubinin–kaganer–radushkevich (DKR)

The DKR isotherm is reported to be more general than the Langmuir and Freundlich isotherms. It helps to determine the apparent energy of adsorption. The characteristic porosity of adsorbent toward the adsorbate and does not assume a homogenous surface or constant sorption potential [32].

The Dubinin–Kaganer–Radushkevich (DKR) model has the linear form

$$\ln q_e = \ln X_m - \beta \varepsilon^2 \quad (12)$$

where X_m is the maximum sorption capacity, β is the activity coefficient related to mean sorption energy, and ε is the Polanyi potential, which is equal to

$$\varepsilon = RT \ln \left(1 + \frac{1}{C_e} \right) \quad (13)$$

where R is the gas constant (kJ/kmol- K) .

The slope of the plot of $\ln q_e$ versus ε^2 gives β (mol^2/J^2) and the intercept yields the sorption capacity, X_m (mg/g) as shown in Fig. 6. The values of β and X_m , as a function of temperature are listed in table 1 with their corresponding value of the correlation coefficient, R^2 . It can be observed that the values of β increase as temperature increases while the values of X_m decrease with increasing temperature.

The values of the adsorption energy, E , was obtained from the relationship [33]

$$E = (-2\beta)^{-1/2}$$

4.4 Thermodynamics parameters for the adsorption

In order to fully understand the nature of adsorption the thermodynamic parameters such as free energy change (ΔG°) and enthalpy change (ΔH°) and entropy change (ΔS°) could be calculated. It was possible to estimate these thermodynamic parameters for the adsorption reaction by considering the equilibrium constants under the several experimental conditions. They can be calculated using the following equations [34]:

$$\Delta G = -R \ln K_d(T) \quad (14)$$

$$\ln K_d = \Delta S/R - \Delta H/RT \quad (15)$$

$$\Delta G = \Delta H - T\Delta S \quad (16)$$

The K_d value is the adsorption coefficient obtained from Langmuir equation. It is equal to the ratio of the amount adsorbed (x/m in mg/g) to the adsorptive concentration (y/a in mg/dm³)

$$K_d = (x/m) \cdot (y/a) \quad (17)$$

These parameters are obtained from experiments at various temperatures using the previous equations. The values of ΔH° and ΔS° are determined from the slope and intercept of the linear plot of ($\ln K_d$) vs. ($1/T$).

In general these parameters indicate that the adsorption process is spontaneous or not and exothermic or endothermic. The standard enthalpy change (ΔH°) for the adsorption process is: (i) positive value indicates that the process is endothermic in nature. (ii) negative value indicates that the process is exothermic in nature and a given amount of heat is evolved during the binding metal ion on the surface of adsorbent. This could be obtained from the plot of percent of adsorption (% C_{ads}) vs. Temperature (T). The percent of adsorption increases with increasing temperature, this indicates for the endothermic processes and the opposite is correct [35]. The positive value of (ΔS°) indicates an increase in the degree of freedom (or disorder) of the adsorbed species.

5. Motivation for the removal and sorption Fe³⁺ ions

In practice from recent studies, the natural zeolite [19], activated carbon [36], olive cake [21], quartz and bentonite [20] and jojoba seeds [37] are used as an adsorbent for the adsorption of mainly trivalent iron ions in aqueous solution. The motivation for the removal and sorption Fe³⁺ ions is that iron ions cause serious problems in the aqueous streams especially at high levels concentration [38 - 39]. Usually, the iron ions dissolve from rocks and soils toward the ground water at low levels, but it can occur at high levels either through a certain geological formation or through the contamination by wastes effluent of the industrial processes such as pipeline corrosion, engine parts, metal finishing and galvanized pipe manufacturing [40 - 41].

The presence of iron at the high-levels in the aqueous streams makes the water unusable for several considerations: Firstly, Aesthetic consideration such as discoloration, the metallic taste even at low concentration (1.8 mg/l), odor, and turbidity, staining of laundry and plumbing fixtures. Secondly, the health consideration where the high level of iron ions precipitates as an insoluble Fe³⁺-hydroxide under an aerobic conditions at neutral or alkaline pH [42]. This can generate toxic derivatives within the body by using drinking

water and can contribute to disease development in several ways. For instance, an excessive amounts of iron ions in specific tissues and cells (iron-loading) promote development of infection, neoplasia, cardiomyopathy, arthropathy, and various endocrine and possibly neurodegenerative disorders. Finally, the industrial consideration such as blocking the pipes and increasing of corrosion. In addition to that, iron oxides promote the growth of micro-organism in water which inhibit many industrial processes in our country [43].

In response to the human body health, its environmental problems and the limitation water sources especially in Jordan [44], the high-levels of Fe^{3+} ions must be removed from the aqueous stream to the recommended limit 5.0 and 0.3 ppm for both inland surface and drinking water, respectively. These values are in agreement with the Jordanian standard parameters of water quality[45]. For tracing Fe^{3+} ions into recommended limit, many chemical and physical processes were used such as supercritical fluid extraction, bioremediation, oxidation with oxidizing agent [46]. These techniques were found not effective due to either extremely expensive or too inefficient to reduce such high levels of ions from the large volumes of water [47 - 48]. Therefore, the effective process must be low cost-effective technique and simple to operate [49 - 52]. It found that the adsorption process using natural adsorbents realize these prerequisites. In addition to that, the natural adsorbents are environmental friend, existent in a large quantities and has good adsorption properties. The binding of Iron(III) ion with the surface of the natural adsorbent could change their forms of existence in the environment. In general they may react with particular species, change oxidation states and precipitate [53]. In spite of the abundant reported researches in the adsorption for the removal of the dissolved heavy metals from the aqueous streams, however the iron(III) ions still has limited reported studies. Therefore our studies are concentrated in this field. From our previous work, the natural zeolite [19], quartz and Bentonite [20], olive cake [21], in addition to the chitin [24], activated carbon [54 - 55] and alumina [56] have been all utilized for this aspect at low levels. The adsorption isotherm models (Langmuir and Freundlich) are used in order to correlate the experimental results.

5.1 Sorption Fe^{3+} ions using natural quartz (NQ) and bentonite (NB)

It is known from the chemistry view that surface of NB and NQ is ending with $(\text{Si-O})^-$ negatively charged. These negative entities might bind metal ions *via* the coordination aspects especially at lower pH values as known in the literatures. Fe^{3+} ions are precipitated in the basic medium. Therefore, the 1 % HNO_3 stock solution is used to soluble Fe^{3+} ions and then achieving the maximum adsorption percentages [20].

The binding of metal ions might be influenced on the surface of NB more than NQ. This is due to the expected of following ideas: (i) NQ have pure silica entity with homogeneous negatively charged, therefore the binding will be homogeneous. (ii) The natural bentonite has silica surface including an inner-layer of alumina and iron oxide, which cause a heterogeneous negatively charged. Therefore, the binding Fe^{3+} ions on the surface on NB might be complicated.

The adsorption thermodynamics modelsof Fe^{3+} ions on NQ and NB at 30 °C are examined [20]. The calculated results of the Langmuir and Freundlich isotherm constants are given in Table 2. The high values of R^2 (>95%) indicates that the adsorption of Fe^{3+} ions onto both NQ and NB was well described by Freundlich

isotherms. It can also be seen that the q_{\max} and the adsorption intensity values of NB are higher than that of NQ. The calculated b values indicate the interaction forces between NB surface and Fe^{3+} ions are stronger than in case of using NQ, this is in agreement with the higher ionic potential of Fe^{3+} . This means that the NB is more powerful adsorbent than NQ. Furthermore, based on this information, we found that the adsorption using NQ and NB is much higher as compared to carbon used by other authors [57].

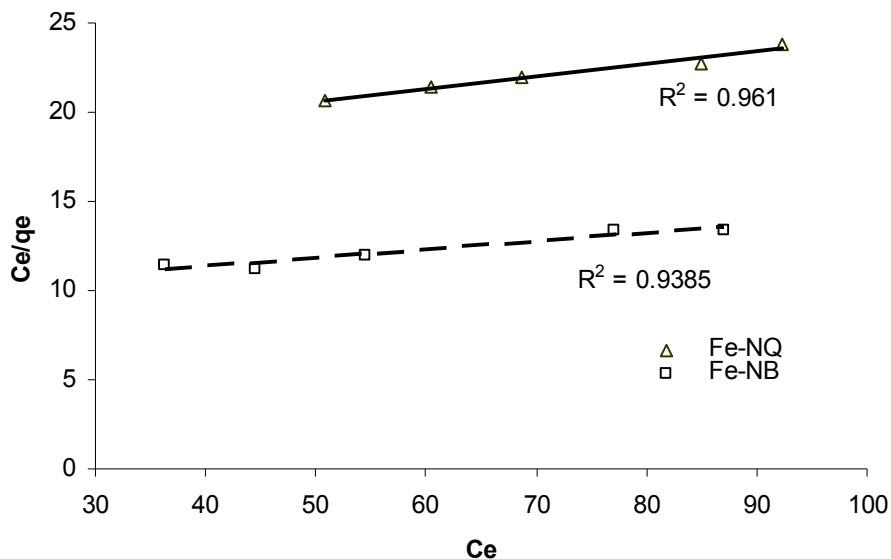


Fig. 5. The linearized Langmuir adsorption isotherms for Fe^{3+} ions adsorption by natural quartz (NQ) and bentonite (NB) at constant temperature 30 °C. (Initial concentration: 400 ppm, 300 rpm and contact time: 2.5 hours).

Langmuir Constants Adsorbent	q_{\max}	b (L/mol)	$\Delta G/1000$ (kJ/mol)
NQ	14.4	226.3	-13.4
NB	20.96	283.8	-13.9

NQ = Natural Quartz

NB = Natural Bentonite

Table 2. Langmuir constants for adsorption of Fe^{3+} ions on NQ and NB

The obtained experimental data also has well described by Freundlich isotherm model into both NQ and NB. The negative value of ΔG° (- 13.4 and - 13.9 KJ/mol, respectively) confirms the feasibility of the process and the spontaneous nature of adsorption with a high preference for metal ions to adsorb onto NB more easily than NQ in pseudo second order rate reaction.

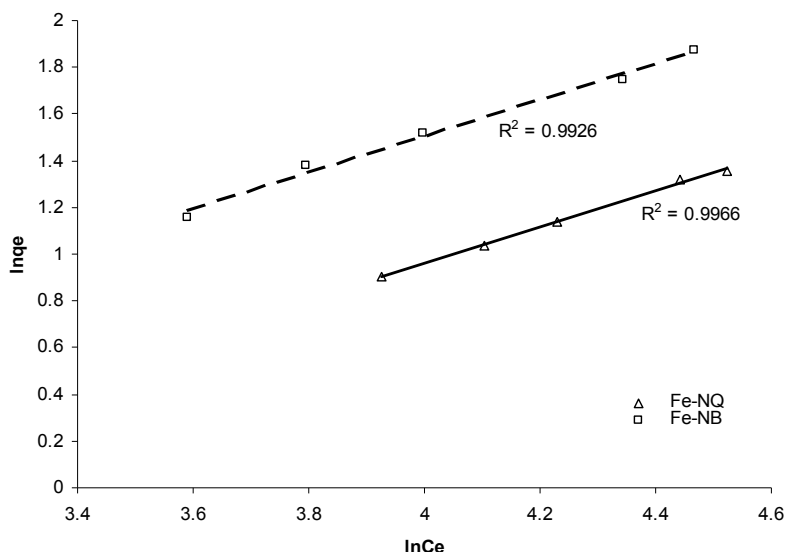


Fig. 6. The linearized Freundlich adsorption isotherms for Fe^{3+} ions adsorption by natural Quartz (NQ) and bentonite (NB) at constant temperature 30 °C. (initial concentration: 400 ppm, normal 1% HNO_3 aqueous solution, 300 rpm, contact time: 2.5 hours).

5.2 Sorption isotherms of Fe^{3+} ions processes using Jordanian natural zeolite (JNZ)

Isotherm studies are conducted at 30 °C by varying the initial concentration of Fe^{3+} ions [19]. Representative initial concentration (1000, 800, 600, 400 ppm) of Fe^{3+} ions are mixed with slurry concentrations (dose) of 20g/L for 150 min., which is the equilibrium time for the zeolite and Fe^{3+} ions reaction mixture. The equilibrium results are obtained at the 1% HNO_3 model solution of Fe^{3+} ions. The Langmuir isotherm model is applied to the experimental data as presented in Figure 7. Our experimental results give correlation regression coefficient, R^2 , equals to 0.998, which are a measure of goodness-of-fit and the general empirical formula of the Langmuir model by

$$\frac{c_e}{q_e} = 0.136c_e + 8.72$$

Our results are in a good qualitatively agreements with those found from adsorption of Fe^{3+} on the palm fruit bunch and maize cob [58].

Figure 8 represents the fitting data into the Freundlich model. We observe that the empirical formula of this model is found as $\ln q_e = 0.1058 \ln C_e + 1.2098$ with R^2 value equals to 0.954. It can be seen that the Langmuir model has a better fitting model than Freundlich as the former have higher correlation regression coefficient than the latter.

The value of standard Gibbs free energy change calculated at 30 °C is found to be -16.98 kJ/mol. The negative sign for ΔG^0 indicates to the spontaneous nature of Fe^{3+} ions adsorption on the JNZ.

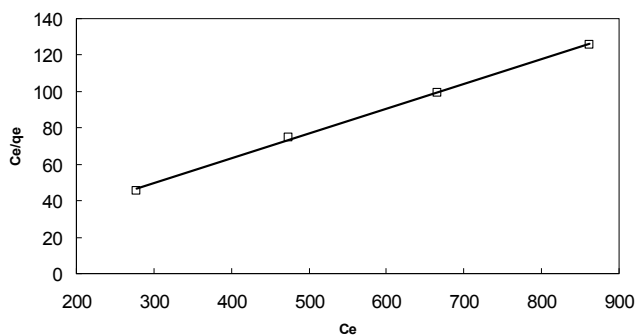


Fig. 7. Langmuir isotherm model plot of q_e/C_e of Fe^{3+} ions on JNZ vs. C_e (ppm) of Fe^{3+} ions.

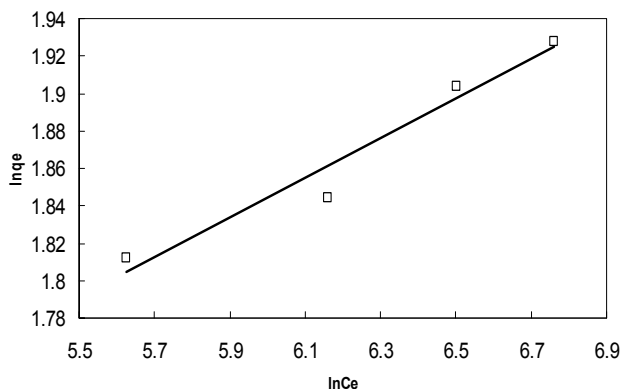


Fig. 8. Freundlich isotherm plot of $\ln q_e$ vs. $\ln C_e$, where C_e is the equilibrium concentration of Fe^{3+} ions concentration.

5.3 Sorption isotherms of Fe^{3+} ions processes using olive cake.

To conduct the isotherm were studied at the initial pH of solution which was adjusted at the optimum value (pH = 4.5) and the mass of olive cake which was taken as 0.3, 0.5, 0.75 and 1.0 g at different temperatures of 28, 35 and 45 °C. Three adsorption isotherms models were used: Langmuir, Freundlich and Dubinin-Kaganer-Radushkevich (DKR) [21]. Figure 9 shows the experimental data that were fitted by the linear form of Langmuir model, (C_e/q_e) versus C_e , at temperatures of 28, 35 and 45 °C. The values of q_{\max} and b were evaluated

from the slope and intercept respectively for the three isothermal lines. These values of q_{max} and b are listed in Table 1 with their uncertainty and their regression coefficients, R^2 . Table 3 shows that the values of q_{max} and b are decreased when the solution temperature increased from 28 to 45 °C. The decreasing in the values of q_{max} and b with increasing temperature indicates that the Fe³⁺ ions are favorably adsorbed by olive cake at lower temperatures, which shows that the adsorption process is exothermic. In order to justify the validity of olive cake as an adsorbent for Fe³⁺ ions adsorption, its adsorption potential must be compared with other adsorbents like eggshells [59] and chitin [24] used for this purpose. It may be observed that the maximum sorption of Fe³⁺ ions on olive cake is approximately greater 10 times than those on the chitin and eggshells.

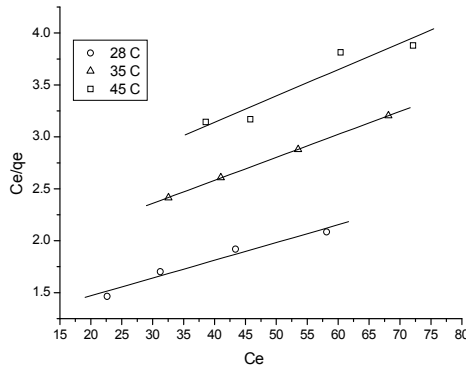


Fig. 9. Langmuir isotherm model plot of q_e/C_e of Fe³⁺ ions on olive cake vs. C_e (ppm) of Fe³⁺ ions.

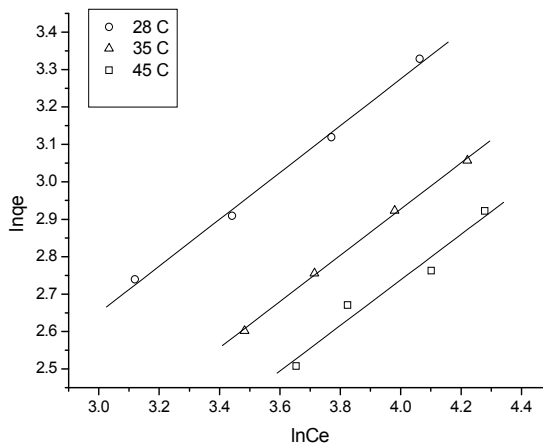


Fig. 10. The linearized Freundlich adsorption isotherms for Fe³⁺ ions adsorption by olive cake at different temperatures. (Initial concentration of Fe³⁺ ions: 100 ppm, Agitation speed: 100 rpm, pH: 4.5, Contact time: 24 hr).

The Freundlich constants K_f and n , which respectively indicating the adsorption capacity and the adsorption intensity, are calculated from the intercept and slope of plot $\ln q_e$ versus $\ln C_e$ respectively, as shown in Figure 10. These values of K_f and n are also listed in Table 3 with their regression coefficients. It can be observed that the values of K_f are decreased with increasing the temperature of solution from 28 to 45 °C. The decreasing in these values with temperature confirms also that the adsorption process is exothermic. It can be also seen that the values of $1/n$ decreases as the temperature increases. Our experimental data of values K_f and $1/n$ are considered qualitatively consistence with those that found in adsorption of Fe^{3+} ions on eggshells [59] and chitin [24].

The negative value of ΔG^0 (Table 4) confirms the feasibility of the process and the spontaneous nature of sorption. The values of ΔH^0 and ΔS^0 are found to be -10.83 kJ/mol and 19.9 J/mol-K, respectively (see Table 4). The negative values of ΔH^0 indicate and exothermic sorption reaction process. The positive value of ΔS^0 shows the increasing randomness at the solid/liquid interface during the sorption of Fe^{3+} ions onto olive cake.

T (°C)	Langmuir			Freundlich			DKR			
	b	q_{\max}	R^2	$1/n$	k_f	R^2	β	X_m	E	R^2
28	0.0152 ± 0.00011	58.479 ± 3.44	0.91	0.626	2.164 ± 0.98	0.99	-0.00006	28.321 ± 1.04	91.287	0.91
35	0.0130 ± 0.00013	45.249 ± 1.17	0.99	0.618	1.578 ± 0.15	0.99	-0.00009	23.539 ± 2.12	74.535	0.97
45	0.012 ± 0.00014	39.370 ± 2.07	0.96	0.609	1.354 ± 0.12	0.96	-0.0001	20.816 ± 1.01	70.711	0.95

Table 3. Langmuir, Freundlich and DKR constants for adsorption of Fe^{3+} ions on olive cake

T(°C)	$b(L/mol)$	$-\Delta G^0$ (kJ/mol)	$-\Delta H^0$ (kJ/mol)	ΔS^0 (J/mol-K)
28	847.2174	16.8718		
35	727.8947	16.8755	10.83	19.9
45	667.7246	17.1953		

Table 4. Thermodynamics parameters for the adsorption of Fe^{3+} ions on olive cake.

5.4 Sorption isotherms of Fe^{3+} ions processes using chitosan and cross-linked chitosan beads

A batch adsorption system was applied to study the adsorption of Fe^{2+} and Fe^{3+} ions from aqueous solution by chitosan and cross-linked chitosan beads [60 - 61]. The adsorption capacities and rates of Fe^{2+} and Fe^{3+} ions onto chitosan and cross-linked chitosan beads were evaluated as shown in Figure 11. Experiments were carried out as function of pH, agitation period, agitation rate and concentration of Fe^{2+} and Fe^{3+} ions. Langmuir and Freundlich

adsorption models were applied to describe the isotherms and isotherm constants. Equilibrium data agreed very well with the Langmuir model.

The calculated results of the Langmuir and Freundlich isotherm constants are given in Table 5. It is found that the adsorptions of Fe^{2+} and Fe^{3+} ions on the chitosan and cross-linked chitosan beads correlated well ($R > 0.99$) with the Langmuir equation as compared to the Freundlich equation under the concentration range studied.

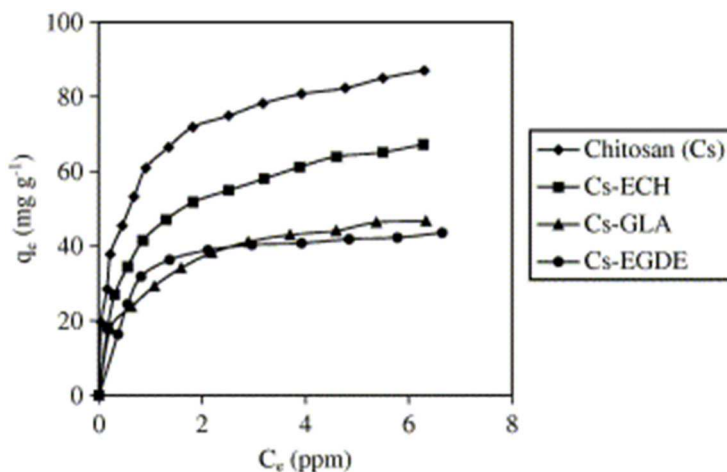


Fig. 11. Adsorption isotherms of Fe^{3+} ions on chitosan and cross-linked chitosan beads. chitosan, chitosan-GLA and chitosan-ECH bead

Iron	Beads	Langmuir			Freundlich		
		Q (mg g^{-1})	b (ml mg^{-1})	R	K_F (mg g^{-1})	n	R
Fe(II)	Chitosan	64.10	2197	0.9986	42.74	4.77	0.7730
	Chitosan-ECH	57.47	1891	0.9998	33.25	3.19	0.9597
	Chitosan-GLA	45.25	1023	0.9995	21.84	2.71	0.9744
	Chitosan-EGDE	38.61	762	0.9985	17.15	2.79	0.9985
Fe(III)	Chitosan	90.09	2413	0.9989	55.27	3.32	0.9824
	Chitosan-ECH	72.46	1550	0.9987	39.35	2.98	0.9788
	Chitosan-GLA	51.55	1405	0.9989	28.63	3.47	0.9881
	Chitosan-EGDE	46.30	2076	0.9991	28.36	3.61	0.8982

Table 5. Langmuir and Freundlich isotherm constants and correlation coefficients

Table 6 lists the calculated results. Based on the effect of separation factor on isotherm shape, the R_L values are in the range of $0 < R_L < 1$, which indicates that the adsorptions of Fe^{2+} and Fe^{3+} ions on chitosan and cross-linked chitosan beads are favourable. Thus, chitosan and cross-linked chitosan beads are favourable adsorbents. As mentioned earlier, chitosan and cross-linked chitosan beads are microporous biopolymers, therefore pores are large enough to let Fe^{2+} and Fe^{3+} ions through. The mechanism of ion adsorption on porous adsorbents may involve three steps [60 - 61]: (i) diffusion of the ions to the external surface of adsorbent; (ii) diffusion of ions into the pores of adsorbent; (iii) adsorption of the ions on the internal

surface of adsorbent. The first step of adsorption may be affected by metal ion concentration and agitation period. The last step is relatively a rapid process.

Iron	Initial concentration (ppm)	R_L value			
		Chitosan	Chitosan-ECH	Chitosan-GLA	Chitosan-EGDE
Fe(II)	3	0.1317	0.1498	0.2457	0.3044
	6	0.0705	0.0810	0.1401	0.1795
	9	0.0481	0.0555	0.0980	0.1273
Fe(III)	3	0.1214	0.1769	0.1917	0.1383
	6	0.0646	0.0971	0.1060	0.0743
	9	0.0440	0.0669	0.0732	0.0508

Table 6. R_L values based on the Langmuir equation

5.5 Adsorption of Fe^{3+} ions on activated carbons obtained from bagasse, pericarp of rubber fruit and coconut shell

The adsorptions of Fe^{3+} ions from aqueous solution at room temperature on activated carbons obtained from bagasse, pericarp of rubber fruit and coconut shell have been studied [62]. The adsorption behavior of Fe^{3+} ions on these activated carbons could be interpreted by Langmuir adsorption isotherm as monolayer coverage. The maximum amounts of Fe^{3+} ions adsorbed per gram of these activated carbons were 0.66 mmol/g, 0.41 mmol/g and 0.18 mmol/g, respectively. The mechanism by which the adsorption of Fe^{3+} ions onto the activated carbon can be performed after being reduced to Fe^{2+} ions [63].

Figures 12 to 14 show the Langmuir plots that have the greatest values of iron adsorption on three types of activated carbons. The maximum adsorption at monolayer coverage on bagasse, pericarp of rubber fruit and coconut shell are in the range 0.25 - 0.66 mmol/g, 0.11 - 0.41 mmol/g and 0.12 - 0.19 mmol/g, respectively. The experimental result shows that the amount of iron ion adsorbed on activated carbons decreased with increasing adsorption temperature. This suggested that the adsorption mechanism was physical adsorption, in contrast to chemical adsorption in which the amount of adsorbate adsorbed on an adsorbent increases with increasing adsorption temperature [63].

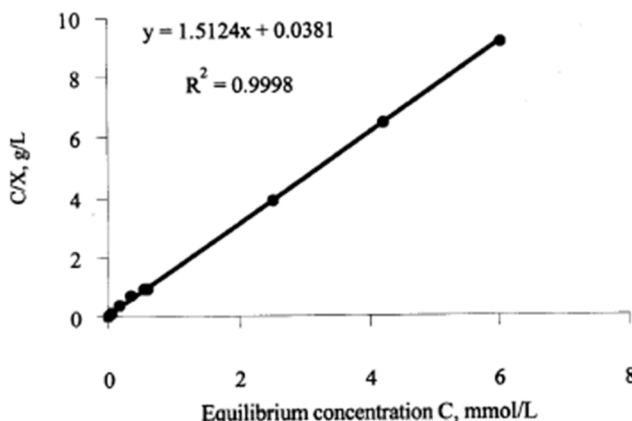


Fig. 12. Langmuir plot for the adsorption of Fe^{3+} ions on activated carbon obtained from bagasse.

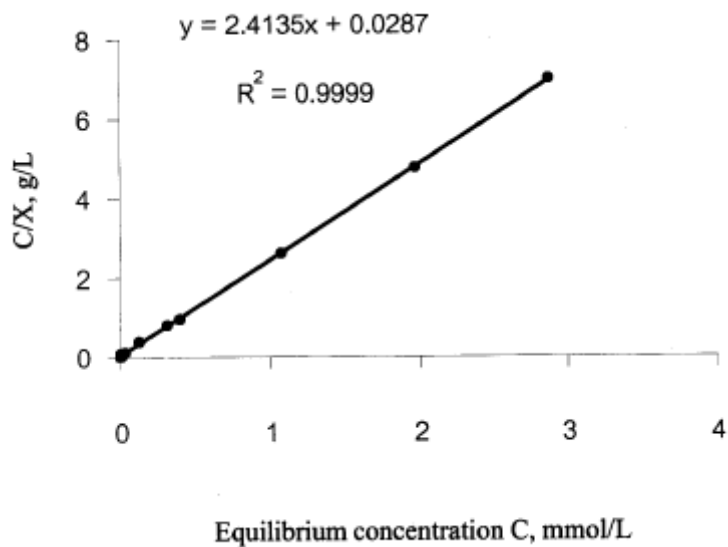


Fig. 13. Langmuir plot for the adsorption of Fe^{3+} ions on activated carbon obtained from pericarp of rubber fruit.

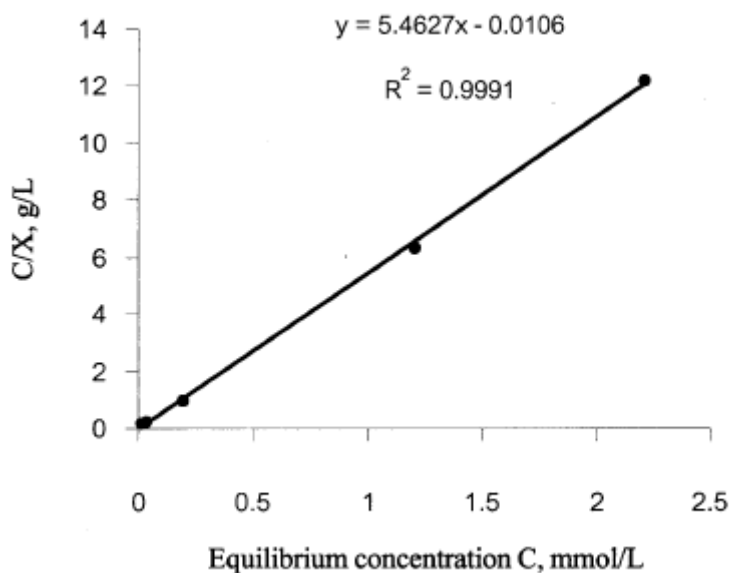


Fig. 14. Langmuir plot for the adsorption of Fe^{3+} ions on activated carbon obtained from coconut shell.

Study of the temperature dependence on these adsorptions has revealed them to be exothermic processes with the heats of adsorption of about -8.9 kJ/mol, -9.7 kJ/mol and -5.7 kJ/mol for bagasse, pericarp of rubber fruit and coconut shell, respectively. The value of Langmuir isotherm constant for the maximum adsorption at monolayer coverage (X_{max}) and the heats of adsorption (ΔH_{ads}) of Fe^{3+} ions on three types of activated carbons was summarized in Table 7.

Raw Materials	X_{max}	ΔH_{ads} (KJ/mol)
Bagasse	0.66	- 8.9
Pericarp of Rubber Fruit	0.41	- 9.7
Coconut Shell	0.19	- 5.7

Table 7. The maximum adsorption of iron ion at monolayer coverage (X_{max}) and the heats of adsorption (ΔH_{ads}) for iron ion on three types of activated carbons and activation temperature at 600 °C

5.6 Adsorption of Fe^{3+} ions on unmodified raphia palm (*Raphia Hookeri*) fruit endocarp

The adsorption of aqueous Fe^{3+} ions onto the surface of *Raphia* palm fruit endocarp (nut) was studied in a batch system [64 – 67]. The influence of initial Fe^{3+} ions concentration, temperature and particle size was investigated and the results showed that particle size and temperature affected the sorption rate and that the adsorption was fast with a maximum percentage adsorption of 98.7% in 20 min as initial metal ion concentration was increased. There is a general decrease in sorption efficiency as the particle size is increased. The increased sorption with smaller particle size means that there is higher external surface area available for adsorption with smaller particle at a constant total mass.

Four isotherms; Langmuir, Freundlich, Dubinin-Radushkevich (D-R) and Temkin were used to model the equilibrium sorption experimental data. The sorption process was found to follow chemisorption mechanism. From Dubinin-Radushkevich (D-R) isotherm, the apparent energy of adsorption was 353.55 KJ/mol. The apparent energy shows if the sorption process follows physisorption, chemisorption or ion exchange. It has been reported:

1. Physisorption processes have adsorption energies <40 KJ/mol
2. Chemisorption processes have adsorption energies > 40 KJ/mol
3. Chemical ion exchange have adsorption energies between 8.0 and 16 KJ/mol
4. Adsorption is physical in nature have adsorption energies <8.0 KJ/mol

From the result obtained, the sorption of Fe^{3+} ions onto *Raphia* palm fruit endocarp (nut) was chemisorption process.

In order to describe the thermodynamic behaviour of the sorption of Fe^{3+} ion onto *Raphia* palm fruit endocarp (nut) from aqueous solution, thermodynamic parameters including ΔG° , ΔH° , ΔS° , were evaluated. The value of ΔH° is negative indicating exothermic process. The standard Gibbs free energy indicates that the the sorption process is spontaneous in nature and also feasible. The decreasing in ΔG° values with increasing temperature shows a decrease in feasibility of sorption at higher temperature.

Isotherm Constants	Fe(III)
Langmuir	- 16.3500
q_{max}	- 0.0800
b	0.9321
R^2	33.1000
$\Delta q(\%)$	
Freundlich	
n	0.6900
K_f	3.9800
R^2	0.9222
$\Delta q(\%)$	8.8100
Dubinin-Radushkevich	
β	$4.0 \cdot 10^{-6}$
q_D	104.4800
E	353.5500
R^2	0.9461
$\Delta q(\%)$	24.5200

Table 9. isotherm constant for adsorption of Fe^{3+} ions onto Raphia palm fruit endocarp (nut) from aqueous solution

Constants (KJ/mol/K)	Fe(III)
ΔH	- 2560.4600
ΔS	19.1900
E_A	2094.8000
S^n	0.0900
R^2 (Vant Hoff)	0.4633
R^2 (Sticking Probability)	0.4747

Table 10. The activation energy of Fe(III)

The activation energy of any reaction process depicts the energy barrier which the reactants must overcome before any reaction could take place. High activation energy to react hence decrease in reaction rate.

6. Conclusion

High and low concentration level of Fe^{3+} ions can be adsorbed on different types of natural adsorbents. This process can be used to remove Fe^{3+} ions from aqueous solutions. The thermodynamic isotherms indicate the behavior picture of Fe^{3+} ions onto the surface of natural adsorbent as homogenous or heterogeneous monolayer coverage. It depends on the chemical nature of adsorbent surfaces. Mostly, the thermodynamic parameters show the spontaneous and exothermic adsorption processes of Fe^{3+} ions onto the surfaces of natural adsorbents, indicating of easier handling.

7. References

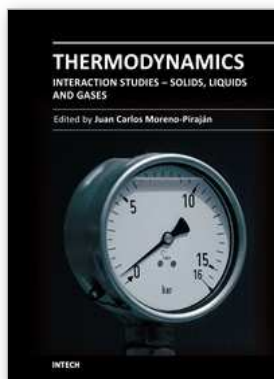
- [1] Sawyer, C. N., and McCarty, P. L. (1978). *Chemistry for environmental engineering*, 3rd Ed., McGraw-Hill, Singapore, 85-90
- [2] Lee, S. H. D., and Johnson, I. J. (1980). "Removal of gaseous alkali metal compounds from hot flue gas by particulate sorbents." *J. Engrg. Power*, 102, 397-402.
- [3] Uberoi, M., and Shadman, F. (1990). "Sorbents for removal of lead compounds from hot flue gases." *AICHE J.*, 36(2), 307-309.
- [4] Ho, T. C., Chen, C., Hopper, J. R., and Oberacker, D. A. (1992). "Metal capture during fluidized bed incineration of wastes contaminated with lead chloride." *Combustion Sci. and Technol.*, 85, 101-116.
- [5] Ho, T. C., Chen, J. M., Shukla, S., and Hopper, J. R. (1990). "Metal capture during fluidized bed incineration of solid wastes." *AICHE Symp. Ser.*, 276(86), 51-60.
- [6] Ho, T. C., Chu, H. W., and Hopper, J. R. (1993). "Metal volatilization and separation during incineration." *Waste Mgmt.*, 13, 455-466.
- [7] Ho, T. C., Tan, T., Chen, C., and Hopper, J. R. (1991). "Characteristics of metal capture during fluidized bed incineration." *AICHE Symp. Ser.*, 281(87), 118-126. a) M.C. Macias-Pbrez, C. Salinas-Martinez de Lecea, M.J. Muiloz- Guillena and A. Linares-Solano, *LOW TEMERATIJJRE SO₂ C A P m BY CALCIUM BASED SORBENTS:CAARACTERIZATION OF THE ACTIVE CALCIUM*. b) MuRoz-Guillena, M.J., Linares-Solano, A. and Salinas-Martinez, de Lecea, C. *Appl. Surf. Sci.*. 1995, 89, 197. Chau-Hwa Yang and James G. Goodwin, Jr., *Journal of Catalysis* 78: 1, 1982, Pages 182-187A. Guerrero-Ruiz, *REACTION KINETICS AND CATALYSIS LETTERS*, 49:1, 53-60, <http://www.webref.org/chemistry/p/physisorption.htm>, International Union of Pure and Applied Chemistry, <http://wikichemistry.com/konfuciy.asp?tda=dt&t=13145&fs=physisorption+-+charactersitics>
- [8] P. Somasundaran, Somil C. Mehta, X. Yu, and S. Krishnakumar, *HANDBOOK OF Surface and Colloid Chemistry*, Third Edition, Colloid Systems and Interfaces Stability of Dispersions through Polymer and Surfactant Adsorption, chapter 6.
- [9] Deguo Kong 2009 , Master Thesis, Department of Land and Water Resources Engineering , Royal Institute of Technology (KTH), SE-100 44 STOCKHOLM, Sweden.
- [10] M. G. Lee, J.K. Cheon, S.K. Kam, *J. Ind. Chem. Eng.* 9(2) (2003) 174-180. a) M. Al-Anber and Z. Al-Anber, Utilization of natural zeolite as ion-exchange and sorbent material in the removal of iron. *Desalination*, 255, (2008) 70 - 81. b) M. Al-anber, Removal of Iron(III) from Model Solution Using Jordanian Natural Zeolite: Magnetic Study, *Asian J. Chem. Vol. 19, No. 5* (2007), 3493-3501.
- [11] A. Guerrero-Ruiz, *REACTION KINETICS AND CATALYSIS LETTERS*, 49:1, 53-60.
- [12] <http://www.webref.org/chemistry/p/physisorption.htm>, International Union of Pure and Applied Chemistry.
- [13] <http://wikichemistry.com/konfuciy.asp?tda=dt&t=13145&fs=physisorption+-+charactersitics>
- [14] P. Somasundaran, Somil C. Mehta, X. Yu, and S. Krishnakumar, *HANDBOOK OF Surface and Colloid Chemistry*, Third Edition, Colloid Systems and

- Interfaces Stability of Dispersions through Polymer and Surfactant Adsorption, chapter 6.
- [15] Deguo Kong 2009 , Master Thesis, Department of Land and Water Resources Engineering , Royal Institute of Technology (KTH), SE-100 44 STOCKHOLM, Sweden.
- a) R.C. Weast, CRC Handbook of Chemistry and Physics, CRC Press, Boca Raton, FL, 1979, p. F-214.]= b) Y. Onganer, C. Temur, Adsorption dynamics of Fe(III) from aqueous solution onto activated carbon, *J. Colloid Interf. Sci.* 205 (1998) 241–244.
- [16] Adil Denizli, Ridvan Say and Yakup Arica Separation and Purification Technology, 21 (2000) 181-190.
- [17] M. G. Lee, J.K. Cheon, S.K. Kam, *J. Ind. Chem. Eng.* 9(2) (2003) 174-180.
- [18] a) M. Al-Anber and Z. Al-Anber, Utilization of natural zeolite as ion-exchange and sorbent material in the removal of iron. *Desalination*, 255, (2008) 70 – 81. b) M. Al-anber, Removal of Iron(III) from Model Solution Using Jordanian Natural Zeolite: Magnetic Study, *Asian J. Chem.* Vol. 19, No. 5 (2007), 3493-3501.
- [19] Mohammad Al-Anber, Removal of High-level Fe³⁺ from Aqueous Solution using Jordanian Inorganic Materials: Bentonite and Quartz, *Desalination* 250 (2010) 885-891.
- [20] Z. Al-Anber and M. Al-Anber, Thermodynamics and Kinetic Studies of Iron(III) Adsorption by Olive Cake in a Batch System, *J. Mex. Chem. Soc.* 2008, 52(2), 108-115.
- [21] Tayel El-Hasan, Zaid A. Al-Anber, Mohammad Al-Anber*, Mufeed Batarseh, Farah Al-Nasr, Anf Ziadat, Yoshigi Kato and Anwar Jiries. Removal of Zn²⁺, Cu²⁺ and Ni²⁺ Ions from Aqueous Solution via Tripoli: Simple Component with Single Phase Model, *Current World Environment*, 3(1) (2008) 01-14
- [22] L.N. Rao, K.C.K. Krishnaiah, A. Ashutosh, *Indian J. Chem. Technol.* 1 (1994) 13.
- [23] G. Karthikeyan, N.M. Andal and K Anbalagan, Adsorption studies of iron(III) on chitin, *J. Chem. Sci.* 117 (6) (2005) 663–672.
- [24] a) N. Khalid, S.Ahmad, S.N. Kiani, J.Ahmed, Removal of mercury from aqueous solutions by adsorption to rice husks, *Sep. Sci. Technol.* 34 (16) (1999) 3139–3153. b) N. Khalid, S. Ahmed, S.N. Kiani, J. Ahmed, Removal of Lead from Aqueous Solutions Using Rice Husk, *Sep. Sci. Technol.* 33 (1998) 2349–2362.
- [25] G. Karthikeyan, N.M. Andal and K Anbalagan, Adsorption studies of iron(III) on chitin, *J. Chem. Sci.* 117 (6) (2005) 663–672.
- [26] *Journal of Research of the National Bureau of Standards—A. Physics and Chemistry*, 66A:6 (1962) 503-515
- [27] N. KANNAN and T. VEEMARAJ, Removal of Lead(II) Ions by Adsorption onto Bamboo Dust and Commercial Activated Carbons -A Comparative Study, *E-Journal of Chemistry*, 2009, 6(2), 247-256.
- [28] I. Langmuir, adsorption of gases on plain surfaces of glass mica platinum, *J. Am. Chem. Soc.* 40 (1918) 136-403. b) J.M. Coulson, J.F. Richardson with J.R. Backhurst, J.H. Harker, (1991) *Chemical Engineering*, Vol 2, 4th Edt. "practical Technology and separation processes" Pergamon Press, Headington Hill Hall, Oxford. c) (Domenico, P.A. and Schwartz, F.W., "Physical and Chemical Hydrogeology", 1st Ed., John Wiley and Sons, New York, 1990). d) Reddi, L.N. and Inyang, H.I., "Geo-

- Environmental Engineering Principles and Applications”, Marcel Decker Inc., New York, 2001. e) Nitzsche, O. and Vereecken, H., “Modelling Sorption and Exchange Processes in Column Experiments and Large Scale Field Studies”. *Mine Water and the Environment*, 21, 15-23, 2002. f) F. Banat, S. Al-Asheh, D. Al-Rousan, A comparative study of copper and zinc ion adsorption on to activated date-pits. *Adsorption Science Technology* 2002, 20 (4) 319-335.
- [29] Vermeulan et al., 1966 T.H. Vermeulan, K.R. Hall, L.C. Eggleton and A. Acrivos *Ind. Eng. Chem. Fundam.* 5 (1966), pp. 212-223.
- [30] a) Metcalf and Eddy. (2003). *Wastewater Engineering, Treatment, Disposal and Reuse*, 3ed Ed. McGraw-Hill: New York. b) Zeldowitsch, 1934 J. Zeldowitsch, Über den Mechanismus der katalytischen Oxydation von CO an MnO₂, *Acta Physicochim. URSS* 1 (1934), pp. 364-449. c) A. EDWIN VASU, *E-Journal of Chemistry*, 5:1, (2008) 1-9.
- [31] Hutson N D, Yang R T, *Adsorption*. 1997, 3, 189. Krishna B S, Murty D S R, Jai Prakash B S, *J. Colloid Interf Sci.* 2000, 229, 230.
- [32] a) Arivoli S, Venkatraman B R, Rajachandrasekar T and Hema M, Adsorption of ferrous ion from aqueous solution by low cost activated carbon obtained from natural plant material, *Res J Chem Environ.* 2007, 17, 70-78. b) Arivoli S, Kalpana K, Sudha R and Rajachandrasekar T, Comparative study on the adsorption kinetics and thermodynamics of metal ions onto acid activated low cost carbon, *E J Chem*, 2007, 4, 238-254. c) Renmin Gong, Yingzhi Sun, Jian Chen, Huijun Liu, Chao yang, Effect of chemical modification on dye adsorption capacity of peanut hull, *Dyes and Pigments*, 2005, 67, 179.
- [33] Jj S Arivoli, P.Martin Deva Prasath and M Thenkuzhali, *EJEAFChe*, 6 (9), (2007) 2323-2340
- [34] O. Sirichote, W. Innajitara, L. Chuenchom, D. Chunchit and K. Naweekan. *Songklanakarin J. Sci. Technol.*, 2002, 24(2) : 235-242.
- M. A. AL-Anber, Z. AL-Anber, I. AL-Momani, *Thermodynamics and Kinetic Studies of Iron(III) Adsorption by Jojoba seeds in a Batch System*, in preparation (2011).
- [35] J. H. Duffus, “Heavy metals”- A Meaningless Term? *IUPAC Technical Report, Pure Appl. Chem.* 74:5 (2002) 793-807.
- [36] E. D. Weinberg, *Iron Loading and Disease Surveillance. Emerging Infectious Diseases*, 5 (3) 1999.
- [37] B. Das, P. Hazarika, G. Saikia, H. Kalita, D.C. Goswami, H.B. Das, S.N. Dube, R.K. Dutta, Removal of iron from groundwater by ash: A systematic study of a traditional method, *Journal of Hazardous Materials* 141 (2007) 834-841.
- [38] a) Gedge G (1992) Corrosion of cast Iron in potable water service. In: *Proceedings of the Institute of Materials Conference*. London, UK. b) Rice, O. Corrosion Control with Calgon. *Journal AWWA*, 39(6), (1947) 552. c) Hidmi, L.; Gladwell, D. & Edwards, M. *Water Quality and Lead, Copper, and Iron Corrosion in Boulder Water. Report to the City of Boulder, CO* (1994).
- [39] J.D. Zuane, *Handbook of Drinking Water Quality*. Van Nostrand Reinhold, New York, 1990.
- a) G. Chen, *Electrochemical technologies in wastewater treatment. Sep. Purif. Technol.* 38 (1), (2004) 11-41. b) M. Wessling-Resnick, *Biochemistry of iron uptake. Crit. Rev. Biochem. Mol. Biol.* 34, (1999) 285-314. c) G. J. Kontoghiorghes and E.D. Weinberg

- Iron: mammalian defense systems, mechanisms of disease, and chelation therapy approaches. *Blood Rev.* 9 (1995) 33-45. d) E.D. Weinberg and G.A. Weinberg. The role of iron in infection. *Current Opinion in Infectious Diseases*, 8 (1995) 164-9. e) E.D. Weinberg, The role of iron in cancer. *Eur. J. Cancer. Prev.* 5 (1996) 19-36. f) J.R. Connor and J.L. Beard, Dietary iron supplements in the elderly: to use or not to use? *Nutrition Today*, 32 (1997) 102-9. j) T-P. Tuomainen, K. Punnonen, K. Nyyssonen, J.T. Salonen. Association between body iron stores and the risk of acute myocardial infarction in men. *Circulation*, 97 (1998) 1461-6. h) J.M. McCord, Effects of positive iron status at a cellular level. *Nutr. Rev.*, 54 (1996) 85-8. i) D. Weinberg, Patho-ecological implications of microbial acquisition of host iron. *Reviews in Medical Microbiology*, 9 (1998) 171-8.
- [40] P. Sarin, V.L. Snoeyink, J. Bebee, K.K. Jim, M. A. Beckett, W.M. Kriven, J. A. Clement, Iron release from corroded iron pipes in drinking water distribution systems, *Water Research*, 38,5, (2004)1259-1269.
- [41] <http://www.unu.edu/unupress/unupbooks/80858e/80858E02.htm>
- [42] F.R. Spellman, *Handbook for Waterworks Operator Certification*, Vol. 2, Technomic Publishing Company Inc., Lancaster, USA, 2001, pp 6-11, 81-83.
- W.C. Andersen, T.J. Bruno, Application of gas-liquid entraining rotor to supercritical fluid extraction: removal of iron (III) from water, *Anal. Chim. Acta* 485 (2003) 1-8.
- [43] a) D. Ellis, C. Bouchard, G. Lantagne, Removal of iron and manganese from groundwater by oxidation and microfiltration, *Desalination* 130 (2000) 255-264. b) Hikmet Katircioglu, Belma Aslim, Ali Rehber Tu'rkcer, Tahir Atic, Yavuz Beyatl, Removal of cadmium(II) ion from aqueous system by dry biomass, immobilized live and heat-inactivated *Oscillatoria* sp. H1 isolated from freshwater (Mogan Lake) *Bioresource Technology* 99 (2008) 4185-4191
- [44] P. Berbenni, A. Pollice, R. Canziani, L. Stabile, F. Nobili, Removal of iron and manganese from hydrocarbon-contaminated groundwaters, *Bioresour. Technol.* 74 (2000) 109-114.
- [45] a) M. Kalin, W.N. Wheeler, G. Meinrath, The removal of uranium from mining waste water using algal/microbial biomass. *J. Environ. Radioact.* 78 (2005) 151-177. b) F. Veglio, F. Beolchini, Removal of metals by biosorption: a review. *Hydrometall.* 44 (1997) 301-316.
- [46] M. Uchida, S. Ito, N. Kawasaki, T. Nakamura, S. Tanada, Competitive adsorption of chloroform and iron ion onto activated carbon fiber, *J. Colloid Interf. Sci.* 220 (1999) 406-409.
- [47] M. Pakula, S. Biniak, A. Swiatkowski, Chemical and electrochemical studies of interactions between iron (III) ions and activated carbon surface, *Langmuir* 14 (1998) 3082-3089.
- [48] C. Huang, W.P. Cheng, Thermodynamic parameters of iron-cyanide adsorption onto -Al₂O₃, *J. Colloid Interf. Sci.* 188 (1997) 270-274.
- [49] a) E. A. Sigworth and S. B. Smith, Adsorption of inorganic compound by activated carbon, *J. Am. Water Works Assoc.*, 64, 386 (1972). b) E. Jackwerth, J. Lohmar and G. Wittler, *Fresenius' Z. Anal. Chem.*, 266, 1(1973). c) A. Edwin Vasu, Adsorption of Ni(II), Cu(II) and Fe(III) from Aqueous Solutions Using Activated Carbon, *E-Journal of Chemistry*, 5 (1), 2008, 1-9. d) A. Ucer, A. Uyanik, S.F. Aygun,

- Adsorption of Cu^{2+} , Cd^{2+} , Zn^{2+} , Mn^{2+} and Fe^{3+} ions by tannic acid immobilised activated carbon, *Separation and Purification Technology* 47 (2006) 113–118.
- [50] Hideko Koshima, Adsorption of Iron(III) on Activated Carbon from Hydrochloric Acid Solution, *Analytical Sciences* (1), 1985, 195.
- [51] a) N. Cvjetićanin, D. Cvjetićanin, D. Golobočanin, and M. Pravica, Adsorption of colloidal trivalent iron on alumina, *J. Radioanalytical and Nuclear Chem.*, 54(1-2), 1979, 149-158.
- [52] A. EDWIN VASU, *E-Journal of Chemistry*, 5:1, (2008) 1-9.
- [53] M.M. Nassar, K.T. Ewida, E.E. Ebrahiem, Y.H. Magdy and M.H. Mheaedi, Adsorption of iron and manganese ions using low-cost materials as adsorbents, *Adsorp. Sci. Technol.*, 22(1) (2004) 25–37.
- [54] Nacèra Yeddou, Aicha Bensmaili, Equilibrium and kinetic modeling of iron adsorption by eggshells in a batch system: effect of temperature, *Desalination* 206 (2007) 127–134.
- [55] W. S. Wan Ngah, S. Ab Ghani and A. Kamari, *Bioresource Technology* Volume 96, Issue 4, March 2005, Pages 443-450.
- [56] Peniche-Covas, C., Alvarez, L.W., Arguelles-Monal, W., 1992. The adsorption of mercuric ions by chitosan. *J. Appl. Polym. Sci.* 46, 1147–1150.
- [57] O. Sirichote, W. Innajitara, L. Chuenchom, D. Chunchit and K. Naweean. *Songklanakarin J. Sci. Technol.*, 2002, 24(2) : 235-242.
- [58] Uchida, M., Shinohara, O., Ito, S., Kawasaki, N., Nakamura, T. and Tanada, S. 2000. Reduction of iron(III) ion by activated carbon fiber. *J. Colloid Interface Sci.* 224: 347-350.
- [59] C.Y. Abasi, A.A. Abia and J.C. Igwe, *Environmental Research Journal*, 5(3), 2011, Page No.: 104-113.
- [60] Y. S. Ho, C. T. Huang, H. W. Huang, equilibrium sorption isotherm for metal ions on tree fern. *Process biochem*, 37 (2002) 1421-1430.
- [61] B. A. Shah, A. V. Shah, R. R> Singh, Sorption isotherms and kinetics of chromium uptake from wastewater using natural sorbent materials. *Intern. J. Environ. Sci. Technology*. 6, (2009) 77-90.
- [62] a) M. Horsfall, A.I. Spiff, A.A. Abia, studies the influence of mercaptoacetic acid (MAA) modification of cassava (*Manihot esculenta* cranz) waste biomass on the adsorption of Cu^{2+} and Cd^{2+} from aqueous solution. *Bull Korean Chem. Soc.* 25 (2004) 969-976. b) P. Loderio, J.L. Barriada, R. Herrero, M.E. Sastre-Vicente, The marine macroalga *Crustoserira baccata* as biosorbent for Cd(II) and Pb(II) removal: kinetic and equilibrium studies. *Environ. Pollution*, 142 (2006) 264-273.



Thermodynamics - Interaction Studies - Solids, Liquids and Gases

Edited by Dr. Juan Carlos Moreno Piraján

ISBN 978-953-307-563-1

Hard cover, 918 pages

Publisher InTech

Published online 02, November, 2011

Published in print edition November, 2011

Thermodynamics is one of the most exciting branches of physical chemistry which has greatly contributed to the modern science. Being concentrated on a wide range of applications of thermodynamics, this book gathers a series of contributions by the finest scientists in the world, gathered in an orderly manner. It can be used in post-graduate courses for students and as a reference book, as it is written in a language pleasing to the reader. It can also serve as a reference material for researchers to whom the thermodynamics is one of the area of interest.

How to reference

In order to correctly reference this scholarly work, feel free to copy and paste the following:

Mohammed A. Al-Anber (2011). Thermodynamics Approach in the Adsorption of Heavy Metals, Thermodynamics - Interaction Studies - Solids, Liquids and Gases, Dr. Juan Carlos Moreno Piraján (Ed.), ISBN: 978-953-307-563-1, InTech, Available from: <http://www.intechopen.com/books/thermodynamics-interaction-studies-solids-liquids-and-gases/thermodynamics-approach-in-the-adsorption-of-heavy-metals>

INTECH

open science | open minds

InTech Europe

University Campus STeP Ri
Slavka Krautzeka 83/A
51000 Rijeka, Croatia
Phone: +385 (51) 770 447
Fax: +385 (51) 686 166
www.intechopen.com

InTech China

Unit 405, Office Block, Hotel Equatorial Shanghai
No.65, Yan An Road (West), Shanghai, 200040, China
中国上海市延安西路65号上海国际贵都大饭店办公楼405单元
Phone: +86-21-62489820
Fax: +86-21-62489821

© 2011 The Author(s). Licensee IntechOpen. This is an open access article distributed under the terms of the [Creative Commons Attribution 3.0 License](#), which permits unrestricted use, distribution, and reproduction in any medium, provided the original work is properly cited.